Cytoplasmic codiffusion of fatty acids is not specific for fatty acid binding protein

BRUCE A. LUXON AND MICHAEL T. MILLIANO
Division of Gastroenterology, Department of Internal Medicine, St. Louis University Health Sciences Center, St. Louis, Missouri 63110-0250

Luxon, Bruce A., and Michael T. Milliano. Cytoplasmic codiffusion of fatty acids is not specific for fatty acid binding protein. *Am. J. Physiol.* 273 (*Cell Physiol.* 42): C859–C867, 1997.—The intracellular movement of fatty acids is thought to be facilitated through codiffusion with fatty acid binding protein (FABP). Previous work suggested that FABP decreases fatty acid binding to immobile membranes, causing faster cytoplasmic diffusion. However, the specificity for binding to FABP has not been addressed. The aim of the current study was to determine whether specific FABP binding is required or whether binding to other proteins will produce the same effect. A model cytoplasm consisted of a fatty acid, proteins, and liposomes to simulate intracellular membranes. Laser photobleaching (fluorescence recovery after photobleaching) was used to measure the movement of the fluorescent fatty acid 12-*N*-methyl-7-nitrobenzo-2-oxa-1,3-diazoaminostearate (NBD-stearate) in model cytoplasm, in normal and permeabilized Hep G2 cells, and after incubation of permeabilized cells with bovine serum albumin (BSA) or FABP. Increasing protein in the model cytoplasm increased the diffusion rate in proportion to the extent of protein binding. Cell permeabilization reduced diffusion of NBD-stearate to <5% of controls. Incubation of permeabilized cells with FABP or BSA resulted in a concentration-dependent increase in the NBD-stearate diffusion rate. BSA was more effective than FABP in binding NBD-stearate and increasing its diffusion rate after permeabilization. Proteins like FABP promote the diffusion of fatty acids. Removal of these proteins drastically reduces cytoplasmic diffusion. Substitution with BSA reestablishes the diffusive flux, suggesting that specific binding to FABP is not required. These data support a role for intracellular binding proteins in facilitating the cytoplasmic movement of fatty acids.

fluorescence recovery after photobleaching; diffusion; liver

LOW-MOLECULAR-WEIGHT cytosolic proteins capable of binding hydrophobic molecules like fatty acids, bile acids, and bilirubin have been studied in hepatocytes, enterocytes, and myocytes for nearly two decades (5, 18). These proteins have been well characterized with regard to their binding affinity for a variety of ligands (2, 25, 30, 32), tissue localization (6, 29), and subcellular distribution (34). However, despite an enormous body of literature, their precise function remains an enigma (5, 18). It has been hypothesized that the intracellular transport and solubility of hydrophobic molecules like fatty acids are facilitated by binding to a group of proteins called fatty acid binding proteins (FABPs). FABPs isolated from different tissues have different protein structures and biochemical properties, including binding affinities for various ligands (32). We use the term FABP to refer to the particular fatty acid binding protein found in hepatocytes (FABP-L) (2). After fatty acids enter the cell, they must be transported through the cytoplasm before they become available to metabolic enzymes. This transport has long been thought to occur by simple diffusion and to be facilitated by binding to FABP. Indirect evidence has suggested that FABP promotes cytoplasmic transport by increasing the amount of fatty acid that is mobile (bound to soluble proteins) and decreasing the amount that is relatively immobile (bound to fixed cytoplasmic membranes). Theoretically, this process would not be specific for FABP binding but should also be observed with other cytosolic proteins that bind fatty acids. Others have suggested that FABP directs fatty acid movement to specific organelles and helps maintain the concentration of fatty acid in the aqueous cytoplasm near key metabolic enzymes (18). For this process to be important, specific binding to FABP would be required, as binding to other proteins would not direct fatty acid movement to special sites of metabolism. Indirect evidence supporting these hypotheses has been obtained using intact perfused livers (3, 4), isolated hepatocytes (9), and cell-free systems (31, 32). Direct experimental evidence supporting a role for FABP in the intracellular transport of fatty acids, however, is lacking.

We previously used the technique of fluorescence recovery after photobleaching (FRAP) to measure the intracellular transport of a fluorescent fatty acid 12-*N*-methyl-7-nitrobenzo-2-oxa-1,3-diazoaminostearate (NBD-stearate) in cultured rat hepatocytes from male and female rats (22, 23). NBD-stearate transport occurred solely by diffusion at a rate that was much slower than expected on the basis of the molecular weight of the NBD-stearate molecule or the NBD-stearate-FABP complex. We hypothesized that this marked retardation of the observed diffusion rate was due to extensive binding to immobile cytoplasmic membranes. The diffusion rate and the fraction of NBD-stearate in the soluble phase of the cytoplasm were greater in female than in male hepatocytes, paralleling the ~1.5- to 2-fold increase in FABP in female cells (22, 23).

We also used another fatty acid analog, α-bromopalmitate, as a competitive inhibitor to displace NBD-stearate from FABP, forcing more of the fluorescent fatty acid to partition into membranes (16, 22). Our results showed that increasing concentrations of α-bromopalmitate caused a progressive decrease in the fraction of NBD-stearate found in the cytosol bound to FABP. This shift in the partition of NBD-stearate between cytosol and membranes correlated closely with the decrease in the transport rate, as measured by laser photobleaching. This finding supported our hypothesis that binding to FABP promotes the intracellular move-

ment of fatty acids by decreasing the amount of fatty acid bound to immobile membranes.

Our previous studies documented experimental evidence for a transport function of cytoplasmic binding proteins such as FABP. However, the issue of protein specificity was not addressed. The current studies are designed to determine whether the facilitation of the intracellular transport of fatty acids is dependent on specific FABP binding or whether binding to other soluble proteins would produce the same effect. To address this issue, we used two systems in which we could readily adjust the composition of binding proteins in the cytoplasm. Initially, we used an in vitro model of the cell cytoplasm that included a fatty acid, various binding proteins, and unilamellar liposomes to simulate intracellular membranes. We measured the partition of native (palmitate) and fluorescent (NBD-stearate) fatty acids between the binding proteins and liposomes and used laser photobleaching to measure the diffusion rate of the fluorescent fatty acid NBD-stearate. Using the technique of cell permeabilization, we then extended this series of experiments to whole cells to allow direct access to the cytoplasm of human hepatoma cells (Hep G2). The binding proteins were introduced into the cytosol of the permeabilized cells, and laser photobleaching was used to measure the rate of intracellular transport.

The results of these experiments indicate that soluble intracellular binding proteins enhance the diffusive flux of fatty acids by modifying the partition between membrane and aqueous phases. Loss of these binding proteins causes nearly all of the NBD-stearate to partition into relatively immobile membranes, and hence the observed cytoplasmic transport rate was drastically reduced. Because replacement of endogenous binding proteins with a noncytosolic protein like bovine serum albumin (BSA) reestablished the diffusive flux of NBD-stearate, we conclude that this facilitation is not specific for FABP. Instead, we suggest that it is a phenomenon of the increase in the fluorescent probe's mobile (aqueous) phase.

These data provide further evidence that small intracellular binding proteins like FABP serve as important carriers of hydrophobic molecules. These binding proteins increase the mobility of a variety of amphipathic and hydrophobic molecules such as long-chain fatty acids by decreasing their binding to membranes. In this manner they can increase the overall utilization of these important metabolic substrates by helping shuttle hydrophobic molecules to their sites of metabolism or excretion.

MATERIALS AND METHODS

Sources of materials. BSA (essentially fatty acid free, catalog no. A3782I), fluorescein isothiocyanate (FITC)-BSA (catalog no. A-9771), and ovalbumin (grade 2, catalog no. A5253) were obtained from Sigma Chemical (St. Louis, MO); NBD-stearate from Molecular Probes (Eugene, OR); and [^{14}C]palmitate (specific activity 57 μCi/μmol) from New England Nuclear (Boston, MA). Culture chambers and coverslips for laser photobleaching experiments (catalog no. 4802) were obtained from Lab-Tek (Los Altos, CA). Capillary tubes made from optical glass (0.2 mm square ID) for FRAP experiments were obtained from Vitro Dynamics (Rockaway, NJ). Streptolysin-O (SLO) was obtained from Murex Diagnostics (Dartford, UK). All other chemicals and reagents were of the highest grade commercially available.

Model cytoplasm using liposomes. Unilamellar negatively charged liposomes composed of phosphatidylcholine (63 μmol), dicetyl phosphate (18 μmol), and cholesterol (9 μmol; kit L4145, Sigma Chemical) were created using standard techniques (26). The size of the liposomes was chosen so that the liposomes themselves did not move by diffusion. They were labeled with [^{3}H]phosphatidylcholine (specific activity 42 Ci/mmol; New England Nuclear). Liposomes were then incubated in Krebs buffer (pH 7.40, 37°C) containing tracer amounts of [^{14}C]palmitate or NBD-stearate and various concentrations of proteins that bind fatty acids (BSA, ovalbumin, and rat FABP-L). The resulting suspension was gently agitated using hand inversion and then allowed to reach equilibrium for 30 min. The partition of [^{14}C]palmitate or NBD-stearate between liposomes and protein was determined by centrifugation at 10,000 *g* for 30 min. Correction was made for nonsedimented liposomes using [^{3}H]phosphatidylcholine. We used these data to estimate the relative affinities of the proteins for NBD-stearate. Specifically, we fit the data to a three-component binding model (free, protein-bound, and membrane-bound NBD-stearate) using nonlinear least-squares regression (see APPENDIX for model equations) (22, 23).

Radiation was detected by liquid scintillation counting with appropriate correction for spillover between ^{14}C and ^{3}H. Fluorescence of NBD-stearate was determined using a dual monochromater spectrofluorometer (model F-1050, Hitachi) with excitation at 488 nm and emission read at 530 nm. For laser photobleaching experiments, small amounts (5–10 μl) of the liposome suspensions containing NBD-stearate were placed in 50-mm-long capillary tubes. After they were filled, the tubes were wiped to remove fluid on the exterior, sealed with wax to prevent evaporation and possible convection, and maintained at 37°C for 10 min before they were used for FRAP studies.

Preparation of FABP. FABP-L was prepared from the cytosolic fraction of livers from female Sprague-Dawley rats (age 45–60 days, weight 200–250 g) using previously published methods (13). Cytosol from the 105,000-*g* supernatant was first pretreated with a Sepharose-anti-albumin column to remove residual albumin and delipidated using a Lidex 1000 column. Large-scale amounts of FABP-L were then prepared exactly as described by Brecher et al. (10) and Dempsey et al. (13).

Cell culture. Hep G2 cells were obtained from the American Type Culture Collection (catalog no. HB 8065) and maintained as previously described (1, 12, 21). Cells (10^6/ml) were plated onto collagen-coated coverslips. Collagen was used because it allowed the Hep G2 cells to spread out and adopt a relatively flat shape for FRAP studies. Cells were maintained at 37°C under an atmosphere of 95% air-5% CO_2 in Ham's Dulbecco's modified Eagle's medium (12400–024, GIBCO BRL, Grand Island, NY). Viability was assessed by trypan blue exclusion before plating and before permeabilization or FRAP use, and preparations were discarded if <85% of the cells excluded the dye.

Measurement of soluble fraction of NBD-stearate in Hep G2 cells. To determine the partition of NBD-stearate between the aqueous cytosol and membranes, Hep G2 cells were removed from culture dishes by trypsinization and suspended in Krebs bicarbonate buffer (8×10^6 cells/ml) containing 1 g/dl BSA and 25 μM NBD-stearate for 20 min. The cells were

separated from the incubation media by low-speed centrifugation (1,000 *g*) for 5 min, and the cell pellet was washed twice with Krebs buffer to remove BSA and resuspended in 10 ml of phosphate-buffered saline (10 mM NaH_2PO_4 and 150 mM NaCl, pH 7.40) at 4°C. The cells were disrupted by homogenization for 15 s. The fluorescence was measured in 1 ml of the cell homogenate. The cytosolic fraction was prepared using centrifugation at 105,000 *g* for 1 h, and the fluorescence was measured in the supernatant. For all fluorescence measurements, care was taken to avoid spurious photobleaching or autoquenching. The fraction of NBD-stearate in the cytosol was expressed as the ratio of the fluorescence in the cytosolic supernatant to that initially present in the cell homogenate (23). NBD-stearate was not metabolized during incubation, as determined by high-performance liquid chromatography of cell cytosol, as previously described (7, 22, 23).

Permeabilization of Hep-G2 cells. Cells were used for permeabilization studies 18 h after plating. Coverslips containing 10^6 cells were incubated in permeabilization buffer [150 mM potassium glutamate and 20 mM piperazine-*N*,*N*′-bis(2-ethanesulfonic acid), pH 6.6] containing 1 IU/ml SLO at 4°C for 30 min. SLO generates persistent membrane lesions large enough to allow proteins up to 300,000 mol wt to efflux from the cell. Because the molecular weight of FABP is ~15,000, previous work suggests that it should efflux from the cell in 20–25 min (33). After 30 min the cells were washed with warm permeabilization buffer (37°C) to initiate permeabilization. Preliminary studies showed that this concentration of SLO was optimal to permeabilize nearly all the Hep G2 cells without causing detachment of cells from the plates (data not shown). The time course of permeabilization was characterized by incubating cells in warm permeabilization buffer containing propidium iodide. Fluorescence due to incorporation of propidium iodide into the nucleus was measured using a fluorometer (SLM Aminco-Bowman, Urbana, IL). We also measured the time course of influx of protein into the permeabilized cells using FITC-BSA. In preliminary experiments the time course for flux of lactate dehydrogenase, aspartate aminotransferase (kit 58–20, Sigma Chemical), and total protein (8) into the media was also determined.

Laser photobleaching. Laser photobleaching (FRAP) was used to measure the diffusion of NBD-stearate in our model cytoplasm and in Hep G2 cells. Studies using Hep G2 cells were done 18 h after plating onto coverslips. Unpermeabilized cells were incubated in Krebs buffer containing 1 g/dl BSA and 25 μM NBD-stearate for 15 min at 37°C. Permeabilized cells were incubated in warm (37°C) permeabilization buffer containing 25 μM NBD-stearate and various concentrations (0, 10, 25, 50, and 150 μM) of BSA or rat hepatic FABP (0, 75, and 150 μM) for 6 min. After incubation, photobleaching experiments were performed as previously described at 37°C (23) using a custom-built video laser photobleaching apparatus. A brief pulse of high-intensity laser illumination was used to irreversibly bleach the NBD-stearate molecules in the selected rectangular area. The bleach beam radius was nominally set at 1.3 μm and was calculated in each experiment as described previously (22, 23). After the bleaching pulse, the recovery of fluorescence in the observation rectangle was detected at time intervals of 0.1–0.5 s for a total of 30–60 s. All fluorescence data, including 5–10 prescans before the bleach pulse, were stored on magnetic disks for subsequent analysis.

Photobleaching data analysis. The cytoplasmic diffusion rate, expressed as an effective diffusion constant (D_{eff}), and the mobile fraction (F_m) of NBD-stearate were determined using a two-step fitting procedure, as previously described (19, 22, 23, 36). Briefly, the fluorescence curves recorded after bleaching were normalized by expressing the fluorescence at each point in the observation rectangle as a fraction of that before the bleach. Each normalized postbleach scan was fitted to a two-dimensional Gaussian function, determining the parameters of the Gaussian distribution using nonlinear least-squares regression (17, 22, 23). Estimates of the diffusion rate constants in the *x*- and *y*-coordinate plane and F_m were obtained by a second nonlinear least-squares fit of the center point of the Gaussian curve as a function of time (17, 19, 22, 23, 36). Convection was detected if the center of the bleach point moved in the *x*-*y* plane. The appropriate diffusion model equations are given in the APPENDIX.

RESULTS

Effect of binding proteins on distribution of NBD-stearate and [^{14}C]palmitate in model cytoplasm. Increasing concentrations of proteins in our model cytoplasm resulted in a shift in the partition of [^{14}C]palmitate or NBD-stearate from the liposomes to the proteins. As shown in Fig. 1 (*left*), this effect was most dramatic for BSA, with >95% of the fatty acid in the cytosol when the BSA concentration was 100 μM. Incubation with ovalbumin and FABP-L also increased the fraction of fatty acid found in the cytosol, but to a lesser extent. For instance, only 18 and 9% of the fatty acid were found in the cytosol when 100 μM ovalbumin or FABP was present. We used these data to estimate the relative affinities of the proteins for NBD-stearate and [^{14}C]palmitate by fitting the data to a three-component binding model. The binding affinities for BSA, ovalbumin, and FABP were 5.09, 0.044, and 0.017 μM^{-1}, respectively. The regression model also estimated the product of the binding affinity and number of binding sites (binding capacity) of the liposomes as 28.4, 27.7,

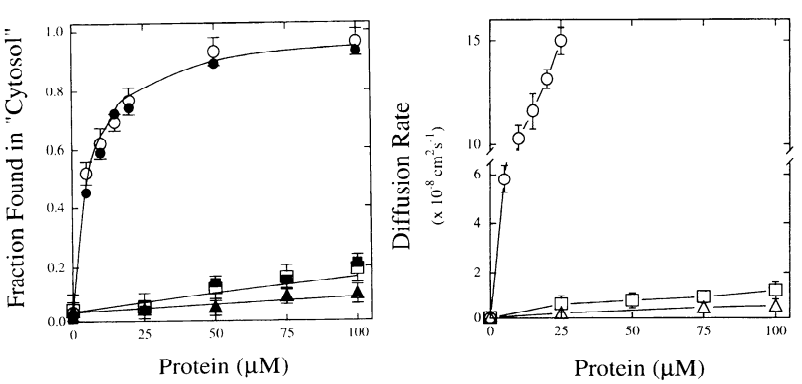

Fig. 1. Effect of binding proteins on fatty acid binding and 12-*N*-methyl-7-nitrobenzo-2-oxa-1,3-diazoaminostearate (NBD-stearate) diffusion in a model of cell cytoplasm. *Left*: increasing concentrations of binding proteins caused a shift in partition of fatty acid from liposomes to protein. NBD-stearate binding to bovine serum albumin (BSA, ○), ovalbumin (□), and fatty acid binding protein (FABP, △) and [^{14}C]palmitate binding to BSA (●), ovalbumin (■), and FABP (▲) are shown. Solid lines, least-squares fit of data to binding model described in APPENDIX. *Right*: diffusion rate of NBD-stearate, as measured using laser photobleaching. ○, BSA; □, ovalbumin; △, FABP. Error bars, SE from 5–15 measurements.

and 28.6, respectively. These latter values were not statistically different. Using this system, we were unable to distinguish any differences in protein binding affinities between [^{14}C]palmitate and NBD-stearate for the three proteins studied (7, 15).

Effect of binding proteins on diffusion of NBD-stearate in model cytoplasm. Increasing the protein concentration in the model cytoplasm caused an increase in the measured diffusion rate of NBD-stearate in proportion to the extent of binding (Fig. 1, *right*). When no protein was present, nearly all the NBD-stearate was bound to liposomes and diffusion was not detectable during the time we used (45–60 s). When BSA was present the measured diffusion rate increased dramatically, reaching a maximum of 15×10^{-8} cm^2/s when 25 μM BSA was present. This value approaches the maximum that can be accurately measured on our photobleaching apparatus given the bleach beam width of 1.3 μm. We were unable to measure the diffusion rate of NBD-stearate when the BSA concentration exceeded 25 μM. The presence of FABP and ovalbumin in the model cytoplasm also increased the observed diffusion rate. At 0–100 μM the observed diffusion rate increased linearly, reaching a maximum of 1.2 and 0.5×10^{-8} cm^2/s for ovalbumin and FABP, respectively.

Because of the different affinities for fatty acids among BSA, ovalbumin, and FABP, it is difficult to infer from Fig. 1 the relationship between the fraction of NBD-stearate found in the cytosol and the diffusion rate of NBD-stearate. When the data of Fig. 1 are combined, it becomes clear that there is a relationship between the cytosolic fraction of NBD-stearate and the diffusion rate (Fig. 2). Over a 100-fold change in the cytosolic fraction, the diffusion rate is in proportion to the fraction of NBD-stearate in the cytosol, regardless of which binding protein is present.

Time course of permeabilization using SLO. Incubation with SLO permeabilized the Hep G2 cells rapidly but predictably. In preliminary experiments we measured the time course of permeabilization in several ways, looking at efflux of lactate dehydrogenase, aspartate aminotransferase, and total protein as well as the influx of propidium iodide and FITC-BSA. Because of the rapidity of permeabilization, the most sensitive technique relied on the change of fluorescence of propidium iodide due to incorporation into cell nuclei. As shown in Fig. 3, permeabilization began almost immediately after warming, with nearly complete permeabilization by 10 min. Control cells exposed to identical buffers and temperatures but without SLO did not show evidence of permeabilization (Fig. 3, control curve). FITC-BSA influx into the permeabilized cells occurred on the same time scale as propidium iodide incorporation into cell nuclei (~5–6 min). No change in intracellular fluorescence intensity due to FITC-BSA occurred over the subsequent 12 min, indicating a stable preparation.

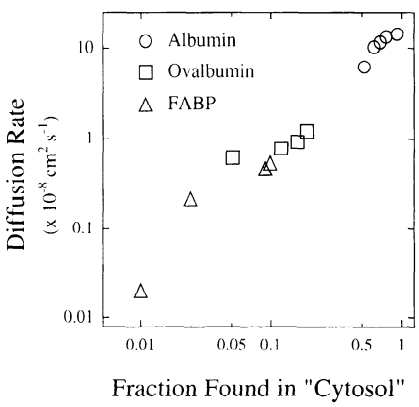

Fig. 2. Relationship between diffusion rate and cytosolic fraction of NBD-stearate in model of cell cytoplasm.

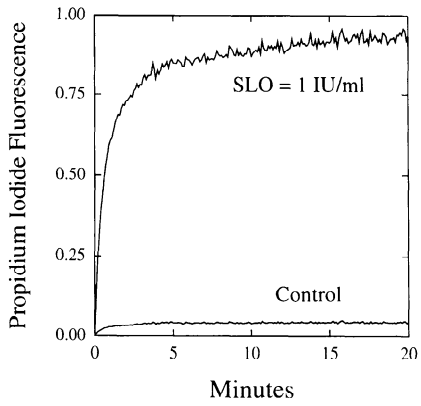

Fig. 3. Time course of permeabilization of Hep G2 cells by streptolysin-O (SLO). Results are from an experiment using a single cell before and after permeabilization.

Quality of fluorescence recovery curve fits. For each bleach study, D_{eff} and F_m were estimated by nonlinear regression. Two representative data sets and their regression curves are shown in Fig. 4. A total of 155 curves were recorded: 72 in control (unpermeabilized) and 83 in permeabilized cells. The average coefficient of determination for these fits was 0.97, with a range of 0.91–0.99. Besides estimating the individual values of D_{eff} and F_m, the fitting algorithm returned their asymptotic standard deviations determined from the information matrix at convergence. The average ratios of the

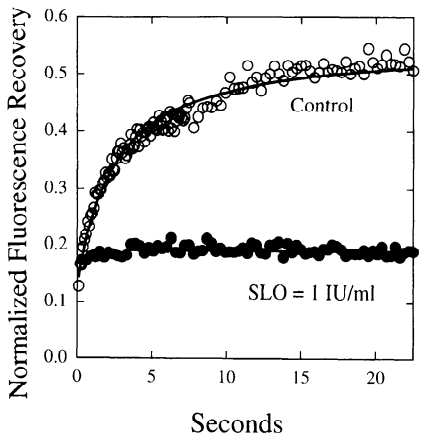

Fig. 4. Fluorescence recovery in permeabilized (*bottom*) and control (*top*) Hep G2 cells. Symbols represent individual data points from a representative experiment. Solid lines, least-squares fit of data to fluorescence recovery model.

standard deviation to the parameter estimate were 0.12 and 0.03 for D_{eff} and F_m, respectively. Permeabilization did not affect the quality of the fits judged by the coefficients of determination or the standard deviations of the estimates of D_{eff} and F_m, although the estimates of the individual parameters changed dramatically (see below).

Gaussian bleach beam. The analysis of fluorescent recovery curves requires knowledge of the cross section of the bleaching beam. For most optical systems, this cross section is described by a Gaussian function (20, 23, 28, 36). Because the absolute value of the measured diffusion constant is critically dependent on this distribution and the beam width, we verified these parameters for each FRAP experiment. The width of the bleach beam was estimated by extrapolation of the width determined from the first three Gaussian functions to zero time. The radius of the beam (measured at $1/e$ of its height) in the experiments reported here was 1.35 ± 0.10 μm, which is consistent with the nominal value of 1.3 μm. Experiments in which the beam width deviated >15% from this value were excluded from further analysis.

Convection and nonhomogeneous diffusion. The technique of laser photobleaching measures the overall movement of fluorescent molecules into the area of observation. This movement could occur by a variety of processes, including simple diffusion, directed diffusion, convection, or a combination of processes (23, 36). Our data analysis algorithm is designed to detect the presence of convection as it locates the minimum of each curve at each time point. However, no convection was detected in any of the recovery curves. The algorithm also detects nonhomogeneous diffusion, i.e., diffusion that proceeds at different rates in different directions. For these studies we measured the diffusion rate of NBD-stearate along two perpendicular lines intersecting at the bleach point. Estimates of the diffusion rate of NBD-stearate were not dependent on direction, with the two directional estimates always being within 11% of each other. Values reported here are therefore the mean of the individual values in the x and y planes. Finally, the diffusion rate did not depend on location within a Hep G2 cell as long as the area of observation did not include the nucleus.

Intracellular diffusion of NBD-stearate. The cytoplasmic transport of NBD-stearate occurred relatively quickly in unpermeabilized cells, with a D_{eff} of $6.7 \pm 0.65 \times 10^{-9}$ cm^2/s ($n = 72$), which is more rapid than that measured in isolated hepatocytes from male ($3.05 \pm 0.21 \times 10^{-9}$ cm^2/s) or female ($5.03 \pm 0.37 \times 10^{-9}$ cm^2/s) rats (22, 23). The fraction of NBD-stearate found in the cytosol in Hep G2 cells was 0.39 ± 0.04 ($n = 13$), which is also greater than that in male (0.18 ± 0.03) or female (0.35 ± 0.07) rat hepatocytes and parallels the increased transport rate of Hep G2 cells. The rate of intracellular movement of NBD-stearate in fully permeabilized cells was reduced to <5% of controls (Figs. 4 and 5). The mean diffusion constant in permeabilized cells in the absence of binding proteins was $0.39 \pm 0.14 \times 10^{-9}$ cm^2/s, which approximates that for the lateral diffusion of fatty acids within membranes, suggesting that nearly all the NBD-stearate is bound to intracellular membranes (14, 36). Incubation of permeabilized cells with BSA or FABP resulted in a concentration-dependent increase in the transport rate of NBD-stearate, reaching prepermeabilization levels in the case of BSA (Fig. 5).

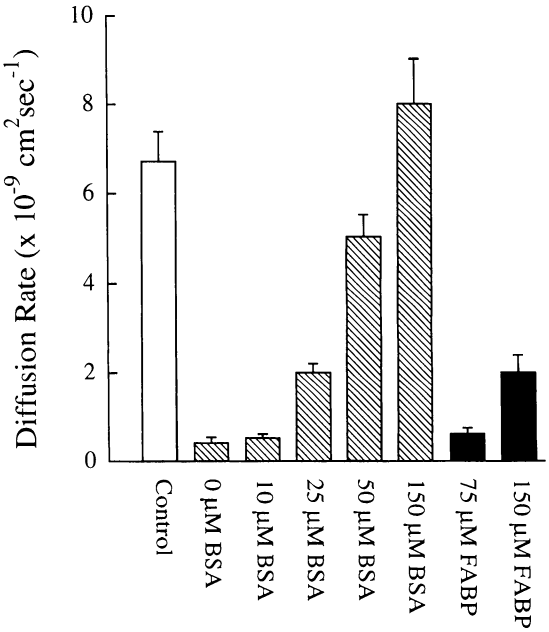

Fig. 5. Loss of cytoplasmic binding proteins reduced diffusion rate of NBD-stearate in permeabilized Hep G2 cells. Replacement of endogenous binding proteins with BSA or FABP reestablished diffusive flux of NBD-stearate. Values are means ± SE, n = 20–72.

DISCUSSION

These results represent measurements of the intracellular diffusion of a fatty acid analog in permeabilized Hep G2 cells in which various binding proteins have been introduced into the cytosol. Previously, we reported measurements of the diffusion rate of NBD-stearate in male and female rat hepatocytes and postulated that FABP enhanced this transport (22, 23). The current studies were designed to further define the possible role of soluble binding proteins like FABP in modulating the intracellular transport of hydrophobic molecules. We wanted to determine whether the enhanced codiffusion of fatty acids with FABP was specific for FABP or whether binding to other soluble proteins such as albumin would produce the same effect.

We postulate that cytoplasmic binding proteins stimulate transport of fatty acids by limiting binding to immobile membranes. The membrane-bound pool of fatty acid contributes little to the diffusional flux for several reasons. First, the membranes themselves do not move (at least on the time scale of our experiments, inasmuch as no convection was detected). Second, cytoplasmic membranes are highly convoluted, a feature that increases the distance a molecule must travel to reach a particular point. Finally, lateral diffusion of fatty acids along the length of the membrane itself is extremely slow (36). For all these reasons, we suggest

that the diffusional flux of fatty acid occurs by movement of the protein-bound pool. We propose that these three pools are in rapid equilibrium (23). We base this on the observation that ~90% of the NBD-stearate was mobile in control Hep G2 cells, yet <39% of the total cytoplasmic NBD-stearate was found in the cytosolic phase. Rapid exchange between these pools is also supported by direct measurement of the "on" and "off" rates for the interaction among fatty acids, membranes, and FABP (31, 32). On the basis of previous work (2, 18, 23, 32), this equilibrium appears to be modulated by the concentration of cytoplasmic binding proteins.

We chose to use a model cytoplasm to study the issue of protein specificity for several reasons. First, the composition of the cytosol could be adjusted, allowing us to study a variety of proteins. Because of the small volume needed to fill the capillary tubes, we needed only microgram amounts of protein for each experiment, minimizing the absolute amount of FABP needed. Second, we wanted to compare the binding of a native fatty acid palmitate with the fluorescent analog NBD-stearate in a simple system devoid of metabolism but containing proteins and membranes. Finally, we were confident that the only mechanism of facilitation in this simple system could be due to a change in the partition of the fatty acid between protein and liposomes.

In our artificial cytoplasm, BSA bound more of the fatty acid and had a much greater effect on the observed diffusion rate of NBD-stearate than FABP or ovalbumin. This is consistent with the reported binding affinities of these proteins for fatty acids. By use of the technique of heptane-water partitioning, these proteins have vastly different binding constants (K_a) for palmitate (F. J. Burczynski, personal communication): 2.2×10^8 M^{-1} for defatted BSA (11, 24), 6.2×10^6 M^{-1} for ovalbumin (11, 24), and 2.1×10^6 M^{-1} for hepatic FABP. As predicted by theory, increasing concentrations of any of the proteins resulted in a shift in the partition of [^{14}C]palmitate from the liposomes to the protein. NBD-stearate and [^{14}C]palmitate had identical binding characteristics in our system, further supporting the use of NBD-stearate as a fatty acid analog, despite the presence of its hydrophobic NBD group (7, 23). Absolute values of D_{eff} for naturally occurring fatty acids may be different from those reported here. However, the relative increases seen with the introduction of binding proteins should still be valid.

Increasing protein concentrations were associated with an increase in the measured diffusion rate of NBD-stearate in proportion to the extent of binding. When no protein was present, nearly all the NBD-stearate was bound to immobile liposomes, and diffusion was not detectable on the time scale we used (30–60 s). When a protein was present, the measured diffusion rate increased dramatically, reaching a maximum when 25 μM albumin was present. Binding to FABP and ovalbumin also increased the observed transport rate, but not to the extent seen with BSA. We suggest that this was due to the relatively diminished (compared with BSA) binding affinities of FABP and ovalbumin. As shown in Fig. 3, this prediction is consistent with our data. There is a constant relationship between the "cytosolic" fraction of NBD-stearate and the observed diffusion rate. Thus, in our model system (as expected), there is no protein specificity for FABP. Instead the enhancement of "cytoplasmic" transport occurs with any protein capable of binding NBD-stearate in proportion to its binding ability. We were unable to determine a protein that did not bind fatty acids to some extent[1] and hence were not able to complete a "negative" control using a completely inert protein in our model system or in permeabilized cells.

We also used the model cytoplasm to determine the lowest detectable magnitude of convection. For these experiments, capillaries were loaded with a combination of liposomes, 10 μM BSA, and NBD-stearate, as described in MATERIALS AND METHODS. However, instead of sealing both ends of the capillary, one end was attached to a microinfusion pump capable of delivering extremely small flow rates with resultant slow convection velocities within the capillary. With this system we were able to accurately detect velocities of 0.625 and 1.25 μm/s (3–5% error, $n = 15$) as well as diffusion. Diffusion rates measured when convection was present were not significantly different from those obtained from sealed capillaries (maximum difference 8%). We are confident therefore that we would have detected convection of this magnitude in our permeabilized cell experiments. Because we did not detect convection in the permeabilized cells, the influx of the binding protein must occur by simple diffusion. We did allow the system to reach equilibrium for 6 min before performing the laser photobleaching experiments. It is unknown whether convection would have been detected immediately after the reconstitution of the cytosol.

Cytoplasmic transport of NBD-stearate was relatively rapid in Hep G2 cells. All this transport occurred by diffusion, as observed in our previous experiments with rat hepatocytes. In unpermeabilized cells the average diffusion rate was $6.7 \pm 0.65 \times 10^{-9}$ cm^2/s ($n = 72$). This is more rapid than the rate observed in hepatocytes obtained from female ($5.0 \pm 0.4 \times 10^{-9}$ cm^2/s) or male ($3.0 \pm 0.2 \times 10^{-9}$ cm^2/s) rats (22, 23). We believe that this rapid rate is due to the more extensive binding of NBD-stearate to soluble proteins in the cytosol of Hep G2 cells. The soluble fraction in the cytoplasm from Hep G2 cells was 0.39 ± 0.07 compared with 0.35 ± 0.07 and 0.18 ± 0.03 in female and male hepatocytes, respectively. As shown by Waggoner (35), Hep G2 cells contain human FABP (molecular weight 14,400), which binds the majority of the fatty acid found in their cytosol. However, Hep G2 cytosol also contains at least two other soluble proteins (molecular weight 24,000 and 35,000) that bind fatty acids (35). The identity of these other proteins has not been determined. Because multiple proteins are involved in cytosolic binding of fatty acids, we chose to measure the

[1] As measured using heptane-water partitioning, lysozyme, hemoglobin, and ferritin have binding affinities (K_a) for palmitate of at least 10^4 M^{-1}.

fraction of fatty acid found in the cytosol rather than the particular protein concentrations. Also slight differences in the binding affinities between rat and human liver FABP further complicate the relationship between protein concentration and bound concentration of fatty acid. Our assay therefore is a functional one that reflects the fraction of fatty acid that we believe is available for rapid diffusion (22, 23).

Permeabilization of Hep G2 cells caused a dramatic decline in the diffusion rate of NBD-stearate to <5% of controls. Values of D_{eff} in fully permeabilized cells are consistent with those reported for the lateral diffusion of fatty acids within membranes (27, 36), suggesting that essentially none of the fluorescent probe is in the aqueous phase. Incubation of permeabilized cells with BSA or rat hepatic FABP resulted in a concentration-dependent increase in the transport rate of NBD-stearate, reaching prepermeabilization levels in the case of BSA. Adding FABP increased the cytoplasmic transport rate, but not to the same extent as adding equimolar concentrations of BSA. This result parallels the findings using our liposome model of the cytoplasm and is consistent with the ~100-fold lower binding affinity of NBD-stearate for FABP than for BSA.

Because replacement of endogenous binding proteins with BSA reestablished the diffusive flux of NBD-stearate, we conclude that facilitation is not specific for FABP. Instead, we suggest that this phenomenon is a function of the increase in the fluorescent probe's aqueous (mobile) concentration. The magnitude of this effect seems to be dependent on the relative binding affinities of the soluble protein and not on the protein itself. These studies were not designed to determine whether codiffusion with FABP delivers the fatty acid preferentially to metabolic sites in intact hepatocytes. Further work is needed to address this issue.

In summary, we have used the technique of laser photobleaching to measure the cytoplasmic transport of a fluorescent fatty acid analog NBD-stearate in a model of the cytoplasm containing fatty acid, various binding proteins, and liposome membranes and in control and permeabilized Hep G2 cells. Each of these systems allowed us to directly manipulate the composition of the cytosol and address the issue of protein specificity of facilitated codiffusion. We conclude from these experiments that soluble binding proteins like FABP enhance the diffusive flux by modifying the partition of fatty acids between membrane and aqueous phases. Loss of binding proteins results in extremely slow cytoplasmic movement, since nearly all the fatty acid partitions into relatively immobile membranes. Because replacement of endogenous binding proteins with BSA reestablished the diffusive flux, we conclude that this facilitation is not specific for FABP but, instead, is a phenomenon solely of the increase in the fatty acid's aqueous concentration. The data obtained in these experiments suggest that small binding proteins like FABP increase the intracellular transport of amphipathic molecules by decreasing their binding to immobile cytoplasmic membranes and may increase the overall utilization rates of these important metabolic substrates by delivering more fatty acids to key metabolic enzymes located throughout the cytoplasm.

APPENDIX

Diffusion model development. The partial differential equation describing homogeneous diffusion in the cytoplasm for a totally mobile fluorophore is given by

$$D\left(\frac{\partial^2 C}{\partial y^2}\right) + D\left(\frac{\partial^2 C}{\partial x^2}\right) - v_x\frac{\partial C}{\partial x} - v_y\frac{\partial C}{\partial y} = \frac{\partial C}{\partial t} \quad (1)$$

where $C(x,y,t)$ is the concentration of fluorophore at position (x,y) at time t, D is the diffusion constant, and v_x and v_y are the x and y components of the convective velocity. These equations are similar to those published previously for "spot" FRAP (22, 23). The initial condition imposed by the Gaussian intensity of the bleaching beam for a "shallow bleach" (8, 14, 28) is

$$C(x,y,t=0) = C_0 + (C_u - C_0) \times \left(1 - \exp - \left\{\frac{-2[x - x_0(0)]^2 + [y - y_0(0)]^2}{R^2}\right\}\right) \quad (2)$$

where R represents the radius ($1/e^2$) of the photobleach and x_0 and y_0 are time-dependent coordinates of the bleach center given by

$$x_0(t) = x_0(t=0) + v_x t$$

$$y_0(t) = y_0(t=0) + v_y t$$

Here C_0 is the concentration of fluorophore at the center of the bleach. The boundary condition is $C(x=\infty, y=\infty, t) = C_u$. The solution to *Eqs. 1* and *2* with this boundary condition can be constructed using a variety of techniques (17) and is given by

$$C(x,y,t) = C_0 + \left[(C_u - C_0)\frac{8Dt}{R^2 + 8Dt}\right] + (C_u - C_0)\left(1 - \exp - \left\{\frac{2[(x - x_0)^2 + (y - y_0)^2]}{R^2 + 8Dt}\right\}\right) \quad (3)$$

From *Eq. 3*, the concentration function simplifies greatly if the x and y values are chosen to be at the time-dependent center of the bleach. If we monitor the fluorescence at the center point of the bleach and denote this function by $C_0(t)$, $C_0(t)$ is given by

$$C_0(t) = C[x_0(t), y_0(t), t] = F_m\left[C_0 + (C_u + C_0)\left(1 - \frac{8Dt}{R^2 + 8Dt}\right)\right] \quad (4)$$

where F_m is the fraction of fluorophore that is mobile over the time course of the experiment. The displacement of the location of the center of the bleach as a function of time was used to measure v_x and v_y.

If nonhomogeneous diffusion occurs, the profile is no longer symmetrical about the x-y axes but, instead, becomes elliptical (17). In this case the postbleach images were fit to

$$C(x,y,t) = F_m\left(C_0(t) + [C_u - C_0(t)] \times \left\{1 - \exp - \left[\frac{2(x - x_0)^2}{R_x^2(t)} + \frac{2(y - y_0)^2}{R_y^2(t)}\right]\right\}\right) \quad (5)$$

where

$$C_0(t) = C_0 + (C_u - C_0)\left[\frac{8D_x t}{R_x^2(t)} + \frac{8D_y t}{R_y^2(t)}\right]$$

$$R_x(t) = R^2 + 8D_x t$$

$$R_y(t) = R^2 + 8D_y t$$

and D_x and D_y are the diffusion rate constants in the x and y planes, respectively.

Fluorescence data were fit to a two-dimensional Gaussian profile (*Eq. 3*) at each time point using nonlinear least-squares regression to determine the location and concentration of the center point and width of the profile. Estimates of D_x, D_y, and F_m were obtained by minimizing the sum of squares between *Eq. 5* and the measured center point concentrations.

Effect of binding. Consider the case where a small transported molecule interacts within the cytoplasm with a mobile binding protein (e.g., FABP) and an immobile substance (e.g., a membrane). If these reactions are rapid with respect to the diffusion process, then a local equilibrium is achieved between the immobile and the mobile species. Let K_1 and K_2 be the equilibrium constants for binding between the free fluorophore (A) and the mobile protein and immobile membrane. If we assume that the total concentration of fluorophore (A_T) is small relative to the total concentration of mobile protein sites (B_T) and membrane sites (C_T), then the equilibrium free fraction of fluorophore (A/A_T) is given by

$$\frac{A}{A_T} = \frac{1}{1 + K_1 B_T + K_2 C_T} \tag{6}$$

Similarly, the fractions bound to the mobile protein and membrane are, respectively

$$\frac{B}{A_T} = \frac{K_1 B_T}{1 + K_1 B_T + K_2 C_T} \tag{7}$$

and

$$\frac{C}{A_T} = \frac{K_2 C_T}{1 + K_1 B_T + K_2 C_T} \tag{8}$$

where B and C are the concentrations of fluorophore bound to the mobile protein and immobile membrane, respectively. The fraction of fluorophore found in the "cytosol" is the sum of free and protein-bound pools

$$\frac{A + B}{A_T} = \frac{1 + K_1 B_T}{1 + K_1 B_T + K_2 C_T} \tag{9}$$

Equation 9 was used to fit the binding data obtained using the model cytoplasm shown in Fig. 1 (*left*).

Hardave Kharbanda assisted in some of these studies as part of a summer fellowship program sponsored by the American Gastroenterological Association. The authors thank Dr. Richard Weisiger for many helpful discussions during the initiation of this project.

B. A. Luxon is a recipient of the Mary Richards Liver Scholar Award from the American Liver Foundation. Portions of this research were funded by awards to B. A. Luxon from the Glaxo Institute of Digestive Health, the Whitaker Foundation for Biomedical Research, and by National Institute of Diabetes and Digestive and Kidney Diseases Grant DK-46922.

Address for reprint requests: B. A. Luxon, PO Box 15250, Div. of Gastroenterology and Hepatology, St. Louis University Health Sciences Center, 3635 Vista Ave. at Grand Blvd., St. Louis, MO 63110-0250.

Received 24 October 1996; accepted in final form 29 April 1997.

REFERENCES

1. **Aden, D., A. Fogel, S. Plotkin, I. Damjanov, and B. Knowles.** Controlled synthesis of HBSAg in a differentiated human liver carcinoma-derived cell line. *Nature* 282: 615–616, 1979.
2. **Bass, N.** The cellular fatty acid binding proteins: aspects of structure, regulation, and function. *Int. Rev. Cytol.* 111: 143–184, 1988.
3. **Bass, N.** Fatty acid-binding protein expression in the liver: its regulation and relationship to the zonation of fatty acid metabolism. *Mol. Cell. Biochem.* 98: 167–176, 1990.
4. **Bass, N., M. Barker, J. Manning, A. Jones, and R. Ockner.** Acinar heterogeneity of fatty acid binding protein expression in the livers of male, female and clofibrate-treated rats. *Hepatology* 9: 12–21, 1989.
5. **Bass, N., R. Kaikaus, and R. Ockner.** Physiology and molecular biology of hepatic cytosolic fatty acid-binding protein. In: *Hepatic Transport and Bile Secretion: Physiology and Pathophysiology*, edited by N. Tavoloni and P. D. Berk. New York: Raven, 1993, p. 421–446.
6. **Bass, N., and J. Manning.** Tissue expression of three structurally different fatty acid binding proteins from rat heart muscle, liver, and intestine. *Biochem. Biophys. Res. Commun.* 137: 929–935, 1986.
7. **Bass, N., J. Manning, and R. Ockner.** Hepatic zonal uptake of a fluorescent fatty acid derivative is determined by velocity and direction of flow (Abstract). *Gastroenterology* 90: 1710, 1986.
8. **Bradford, M.** A rapid and sensitive method for the quantitation of microgram quantities of protein utilizing the principle of protein-dye binding. *Anal. Biochem.* 72: 248–254, 1976.
9. **Brandes, R., R. Kaikaus, N. Lysenko, R. Ockner, and N. Bass.** Induction of fatty acid binding protein by peroxisome proliferators in primary hepatocyte cultures and its relationship to the induction of peroxisomal beta-oxidation. *Biochim. Biophys. Acta* 1034: 53–61, 1990.
10. **Brecher, P., R. Saouaf, J. Sugarman, D. Eisenberg, and K. Larosa.** Fatty acid transfer between multilamellar liposomes and fatty acid binding proteins. *J. Biol. Chem.* 259: 13395–13401, 1984.
11. **Burczynski, F. J., Z. Cai, J. Moran, and E. L. Forker.** Palmitate uptake by cultured hepatocytes: albumin binding and stagnant layer phenomena. *Am. J. Physiol.* 257 (*Gastrointest. Liver Physiol.* 20): G584–G593, 1989.
12. **Darlington, G., J. Key, and G. Buffone.** Growth and hepatospecific gene expression of human hepatoma cells in a defined medium. *In Vitro Cell. Dev. Biol.* 23: 349–354, 1987.
13. **Dempsey, M., K. E. McCoy, H. Baker, R. Vafradori, T. Lorsbach, and J. Howard.** Large scale purification and structural characterization of squalene and sterol carrier protein. *J. Biol. Chem.* 256: 1867–1873, 1981.
14. **Dupou, L., A. Lopez, and J. Tocanne.** Comparative study of the lateral motion of extrinsic probes and anthracene-labeled constitutive phospholipids in the plasma membrane of Chinese hamster ovary cells. *Eur. J. Biochem.* 7: 669–674, 1988.
15. **Fitz, J., N. Bass, and R. Weisiger.** Hepatic transport of a fluorescent stearate derivative: electrochemical driving forces in intact rat liver. *Am. J. Physiol.* 261 (*Gastrointest. Liver Physiol.* 24): G83–G91, 1991.
16. **Goresky, C., D. Daly, S. Mishkin, and I. Arias.** Uptake of labeled palmitate by the intact liver: role of intracellular binding sites. *Am. J. Physiol.* 234 (*Endocrinol. Metab. Gastrointest. Physiol.* 3): E542–E553, 1978.
17. **Jain, R., R. Stock, S. Chary, and M. Rueter.** Convection and diffusion measurements using fluorescence recovery after photobleaching and video image analysis: in vitro calibration and assessment. *Microvasc. Res.* 39: 77–93, 1990.
18. **Kaikaus, R., N. Bass, and R. Ockner.** Functions of fatty acid binding proteins. *Experientia* 46: 617–630, 1990.
19. **Kaufman, E., and R. Jain.** Quantification of transport and binding parameters using fluorescence recovery after photo-

bleaching: potential for in vivo applications. *Biophys. J.* 58: 873–885, 1990.

20. **Kaufman, E., and R. Jain.** Measurement of mass transport and reaction parameters in bulk solution using photobleaching. *Biophys. J.* 60: 596–610, 1991.
21. **Knowles, B., C. Howe, and D. Aden.** Human hepatocellular carcinoma cell lines secrete the major plasma proteins and hepatitis B surface antigen. *Science* 209: 497–499, 1980.
22. **Luxon, B. A.** Inhibition of binding to fatty acid binding protein reduces the intracellular transport of fatty acids. *Am. J. Physiol.* 271 (*Gastrointest. Liver Physiol.* 34): G113–G120, 1996.
23. **Luxon, B. A., and R. Weisiger.** Sex differences in intracellular fatty acid transport: role of cytoplasmic binding proteins. *Am. J. Physiol.* 265 (*Gastrointest. Liver Physiol.* 28): G831–G841, 1993.
24. **Moran, J., F. J. Burczynski, R. Cheek, T. Bopp, and E. L. Forker.** Protein binding of palmitate measured by transmembrane diffusion through polyethylene. *Anal. Biochem.* 167: 394–399, 1987.
25. **Nemecz, G., T. Hubbell, J. Jefferson, J. Lowe, and F. Schroeder.** Interaction of fatty acids with recombinant rat intestinal and liver fatty acid-binding proteins. *Arch. Biochem. Biophys.* 286: 300–309, 1991.
26. **New, R.** *Liposomes: A Practical Approach.* New York: Oxford University Press, 1990, p. 33–104.
27. **Peters, R., J. Peters, K. Tews, and W. Bahr.** A microfluorimetric study of translational diffusion in erythrocyte membranes. *Biochim. Biophys. Acta* 367: 282–294, 1974.
28. **Qian, H., M. Sheetz, and E. Elson.** Single particle tracking: analysis of diffusion and flow in two-dimensional systems. *Biophys. J.* 60: 910–921, 1991.
29. **Shields, H., M. Bates, N. Bass, C. Best, D. Alpers, and R. Ockner.** Light microscopic immunocytochemical localization of hepatic and intestinal types of fatty acid-binding proteins in rat small intestine. *J. Lipid Res.* 27: 549–557, 1986.
30. **Storch, J.** A comparison of heart and liver fatty acid-binding proteins: interactions with fatty acids and possible functional differences studied with fluorescent fatty acid analogues. *Mol. Cell. Biochem.* 98: 141–147, 1990.
31. **Storch, J., and N. Bass.** Transfer of fluorescent fatty acids from liver and heart fatty acid-binding proteins to model membranes. *J. Biol. Chem.* 265: 7827–7831, 1990.
32. **Storch, J., N. Bass, and A. Kleinfeld.** Studies of the fatty acid-binding site of rat liver fatty acid-binding protein using fluorescent fatty acids. *J. Biol. Chem.* 264: 8708–8713, 1989.
33. **Tatham, P., and B. Gomperts.** Cell permeabilization. In: *Peptide Hormones—A Practical Approach*, edited by K. Siddle and J. Hutton. Oxford, UK: IRL, 1990, vol. 2, p. 257–269.
34. **Unterberg, C., T. Börchers, P. Hojrup, P. Roepstorff, J. Knudsen, and F. Spener.** Cardiac fatty acid-binding proteins. Isolation and characterization of the mitochondrial fatty acid-binding protein and its structural relationship with the cytosolic isoforms. *J. Biol. Chem.* 265: 16255–16261, 1990.
35. **Waggoner, D., J. Manning, N. Bass, and D. Bernlohr.** In situ binding of fatty acids to the liver fatty acid binding protein: analysis using 3-[^{125}I]iodo-4-azido-*N*-hexadecylsalicylamide. *Biochem. Biophys. Res. Commun.* 180: 407–415, 1991.
36. **Yguerabide, J., J. Schmidt, and E. Yguerabide.** Lateral mobility in membranes as detected by fluorescence recovery after photobleaching. *Biophys. J.* 39: 69–75, 1982.